Computational and Structural Biotechnology Journal 21 (2023) 74–85

COMPUTATIONAL AND STRUCTURAL BIOTECHNOLOGY JOURNAL

journal homepage: www.elsevier.com/locate/csbj

# Landscape of the intratumroal microenvironment in bladder cancer: *Implications for prognosis and immunotherapy*

Zichen Bian [a,1], Jia Chen [a,1], Chang Liu [a], Qintao Ge [a], Meng Zhang [a,b], Jialin Meng [a,*], Chaozhao Liang [a,*]

[a] *Department of Urology, The First Affiliated Hospital of Anhui Medical University, Institute of Urology & Anhui Province Key Laboratory of Genitourinary Diseases, Anhui Medical University, Hefei 230022, China*

[b] *Urology Institute of Shenzhen University, The Third Affiliated Hospital of Shenzhen University, Shenzhen University, China*

ARTICLE INFO

*Article history:*
Received 9 September 2022
Received in revised form 25 November 2022
Accepted 25 November 2022
Available online 1 December 2022

*Keywords:*
Bladder cancer
Genomic
Immunotherapy
Overall survival

ABSTRACT

*Introduction:* This study aims to present the landscape of the intratumoral microenvironment and by which establish a classification system that can be used to predict the prognosis of bladder cancer patients and their response to anti-PD-L1 immunotherapy.

*Methods:* The expression profiles of 1554 bladder cancer cases were downloaded from seven public datasets. Single-sample gene set enrichment analysis (ssGSEA), univariate Cox regression analysis, and meta-analysis were employed to establish the bladder cancer immune prognostic index (BCIPI). Extensive analyses were executed to investigate the association between BCIPI and overall survival, tumor-infiltrated immunocytes, immunotherapeutic response, mutation load, *etc*.

*Results:* The results obtained from seven independent cohorts and meta-analyses suggested that the BCIPI is an effective classification system for estimating bladder cancer patients' overall survival. Patients in the BCIPI-High subgroup revealed different immunophenotypic outcomes from those in the BCIPI-Low subgroup regarding tumor-infiltrated immunocytes and mutated genes. Subsequent analysis suggested that patients in the BCIPI-High subgroup were more sensitive to anti-PD-L1 immunotherapy than those in the BCIPI-Low subgroup.

*Conclusions:* The newly established BCIPI is a valuable tool for predicting overall survival outcomes and immunotherapeutic responses in patients with bladder cancer.



## 1. Introduction

Bladder cancer is deemed one of the ten most frequent malignancies worldwide, with an estimated 83,730 new cases and 17,200 deaths yearly in the United States [1]. Although the disease is curable in the early stages with surgery, few treatment options are available for patients with metastatic diseases, whose five-year overall survival rate remains at approximately 15 % [2]. An increasing body of evidence suggests that the crosstalk between tumor cells and the tumor microenvironment plays a critical role in tumor cell growth, invasion, and metastasis [3]. In addition, immunocytes in the microenvironment can exert either tumor-suppressing or tumor-promoting effects, which will lead to diverse clinical outcomes.

The tumor-infiltrating immunocytes within bladder cancer tissues have been identified and characterized by investigations for a long time. The existence of $CD8^+$ tumor-infiltrating lymphocytes is correlated with ameliorative outcomes in patients with muscle-invasive urothelial carcinoma, while the abundance of immunosuppressive regulatory T cells (Tregs) and macrophages is associated with compromised survival outcomes [4]. Patients with tumors characterized by low Tregs, low $CD68^+$/$CD163^+$ macrophages, and high $CD4^+$ T cells primarily have a favorable prognosis in response to Bacillus Calmette–Guerin (BCG) therapy [5]. In addition, bladder cancer is the only solid malignancy in addition to

*Abbreviations:* BCG, Bacillus Calmette-Guerin; FDA, Food and Drug Administration; CNVs, Copy number variations; MES, Mesenchymal transition; AJCC, American Joint Committee on Cancer; ICI, Immune checkpoint inhibitor; Anti-PD-L1, Antitumor response to atezolizumab; FPKM, Fragments per kilobase per million; TPM, Transcripts per kilobase million; RMA, Robust multiarray average; ssGSEA, Single-sample GSEA; NES, Normalized enrichment score; BCIPI, Bladder cancer immune prognostic index; IHC, Immunohistochemistry; RMS, Restricted mean survival.

* Corresponding authors at: Jixi Road 218, Shushan District, Hefei City 230022, Anhui Province, China.

*E-mail addresses:* mengjialin@ahmu.edu.cn (J. Meng), liang_chaozhao@ahmu.edu.cn (C. Liang).

[1] These authors contributed equally to the work.

https://doi.org/10.1016/j.csbj.2022.11.052

melanoma, and immunotherapy offers survival benefits. The US Food and Drug Administration (US FDA)-approved immunotherapeutic agents targeting PD-1 or PD-L1 have demonstrated prolonged stable effects among metastatic bladder cancer patients [6]. It should be highlighted here that the immunotherapeutic efficacy of many tumors, including bladder cancer, is correlated with the tumor immune microenvironment, neoantigens, copy number variations (CNVs), and tumor mutational burden [7–10].

This study aimed to establish a novel classification index by comprehensively collecting infiltrated immunocyte/immune response-related signatures and then exploring the correlation between the bladder cancer immune microenvironment and cancer genotypes.

## 2. Methods

### 2.1. Patient summary

Bladder cancer tissue arrays were purchased from Shanghai Outdo Biotech Company Ltd. (Shanghai, China). Ethical approval was obtained from the ethics committees of the company and the First Affiliated Hospital of Anhui Medical University (Approval Number: PJ2021-08-30). A total of 888 bladder patients with complete clinical features and available follow-up information were enrolled from four public datasets, namely The Cancer Genome Atlas Bladder Cancer (TCGA-BLCA, n = 403), GSE31684 (n = 93), GSE32894 (n = 224), and GSE13507 (n = 165) cohorts. And 669 patients from other three public cohorts named GSE32548 (n = 130), GSE48075 (n = 63), and E-MTAB-4321 (n = 476) were used for the external validation. The demographic and clinicopathological features of the enrolled patients are summarized in Table 1.

### 2.2. Data preprocessing

Raw count data was obtained from high-throughput sequencing in the TCGA-BLCA cohort. The fragments per kilobase per million (FPKM) were computed based on the raw count data and then transformed into transcripts per kilobase million (TPM) values. In addition, we filtered these mRNAs whose TPM values were less than 1 in more than 90 % of cases. For microarray data obtained from the GEO datasets (GSE31684, GSE32894, and GSE13507), we used the R package affy to perform robust multiarray average (RMA) normalization [11]. The original gene expression data were log2 transformed and median-centered for subsequent analysis. A detailed description of the platform and the download links for each cohort are listed in Supplementary Table 1.

### 2.3. Collection of immunocyte/immune response-related signatures and single-sample gene set enrichment analysis (ssGSEA)

After comprehensive retrieval, we collected 162 immunocyte/immune response-related signatures [7,12–36]. Repeated signatures were recombined by enrolling all available genes. In addition, we used the R packages clusterProfiler and GSVA to perform GSEA [37] and ssGSEA [38,39], respectively. The normalized enrichment score (NES) of the 162 immune-related signatures in each case was obtained through ssGSEA; for the calculation of each signature, missing expression data for less than five genes were allowed.

### 2.4. Establishment of the bladder cancer immune prognostic index (BCIPI)

The tumor immune infiltration level of each case was evaluated through the NES score derived from ssGSEA. Then, univariate Cox regression analysis was executed to identify overall survival-related signatures. Meta-analyses were performed to further synthesize the hazard ratios of each signature in the four independent cohorts based on the fixed-/random-effect model referring to the heterogeneity analysis. These signatures, whose synthesized *P* value was less than or equal to 0.05, were enrolled to establish the BCIPI using the following equation:

$$\mathrm{BCIPI} = \sum_{i=1}^{n} NES_i - \sum_{j=1}^{n} NES_j$$

*NESi* is defined as the normalized ssGSEA score for the $i^{\mathrm{th}}$ immune-related signature in which the synthesized hazard ratio (HR) value was higher than 1, and *NESj* is defined as signatures in which the synthesized HR value was less than 1.

### 2.5. Correlation of the BCIPI with immunocyte infiltration, immune checkpoints, and response to immunotherapy

The R package “estimate” generated a tumor purity index and immune score that could reflect the immune infiltration status [40]. Charoentong et al. [41] reported using ssGSEA based on 28 gene sets to assess the infiltration abundance of 28 immunocytes. We also evaluated the expression of 66 immune checkpoints with different BCIPIs in the four independent cohorts using the Pearson correlation test. To predict the response of the BCIPI subgroup to anti-PD-L1 immunotherapy, we downloaded the expression profiles of bladder cancer patients in the IMvigor210 cohort from the R package IMvigor210CoreBiologies (http://research-pub.gene.com/IMvigor210CoreBiologies), which comprised a set of patients with locally advanced and metastatic diseases receiving atezolizumab (anti-PD-L1) treatment [7]. The GenePattern module SubMap was used to compare the similarities and differences between BCIPI subgroups in the four bladder cancer cohorts and anti-PD-L1 responders in the IMvigor210 cohort [42].

### 2.6. Correlation of the BCIPI with copy number alterations and gene mutation

GISTIC2.0 was applied to generate CNV data from GDAC Firehose (https://gdac.broadinstitute.org). We compared the differences between the BCIPI-H and BCIPI-L subgroups at the focal level of amplification/deletion and arm level of amplification/deletion. In addition, the mutation matrix of the TCGA cohort was obtained from the GDC website using the TCGAbiolinks R package [43]. We used the R package maftools to plot the Oncoprint for the BCIPI-H and BCIPI-L subgroups [44].

### 2.7. Correlation of the BCIPI with published molecular subtypes

The TCGA group proposed a new molecular classification system that includes luminal-papillary, luminal-infiltrated, luminal, basal/squamous, and neuronal [45]. In addition, Thorsson et al. [46] proposed six pancancer immune subtypes, including TGF-β dominant, IFN-γ dominant, lymphocyte depleted, wound healing, inflammatory, and immunologically quiet. Therefore, the correlation between BCIPI subgroups and these previously defined molecular subtypes was analyzed.

### 2.8. Immunohistochemistry (IHC) validation

An IHC assay was performed to validate the identified immunocytes, such as macrophages (CD163, ab87099, MA, USA). The proportions of $CD8^+$ and $PD\text{-}L1^+$ cells were provided by Shanghai Outdo Biotech Company Ltd (Shanghai, China). The IHC assay was carried out according to the procedure reported in our previ-

**Table 1**
Basic clinicopathological features of enrolled cohorts.

| | TCGA-BLCA (N = 403) | GSE13507 (N = 165) | GSE31684 (N = 93) | GSE32894 (N = 224) | GSE32548 (N = 130) | GSE48075 (N = 63) | E-MTAB-4321 (N = 476) |
|---|---|---|---|---|---|---|---|
| **Age, years old** | | | | | | | |
| Mean (SD) | 67.9 (10.5) | 65.2 (12.0) | 69.1 (10.2) | 69.4 (11.3) | 69.7 (10.6) | 67.8 (9.72) | 68.9 (10.9) |
| Median [Min, Max] | 69.0 [34.0, 89.0] | 66.0 [24.0, 88.0] | 69.2 [41.7, 91.1] | 70.0 [20.0, 93.0] | 70.5 [38.0, 90.0] | 68.0 [42.7, 86.2] | 69.5 [23.5, 95.5] |
| **Gender** | | | | | | | |
| Female | 105 (26.1 %) | 30 (18.2 %) | 25 (26.9 %) | 61 (27.2 %) | 31 (23.8 %) | 0 (0 %) | 109 (22.9 %) |
| Male | 298 (73.9 %) | 135 (81.8 %) | 68 (73.1 %) | 163 (72.8 %) | 99 (76.2 %) | 0 (0 %) | 367 (77.1 %) |
| unknown | 0 (0 %) | 0 (0 %) | 0 (0 %) | 0 (0 %) | 0 (0 %) | 63 (100 %) | 0 (0 %) |
| **Tstage** | | | | | | | |
| CIS | 0 (0 %) | 0 (0 %) | 0 (0 %) | 0 (0 %) | 0 (0 %) | 0 (0 %) | 3 (0.6 %) |
| Tis | 0 (0 %) | 0 (0 %) | 0 (0 %) | 0 (0 %) | 0 (0 %) | 1 (1.6 %) | 0 (0 %) |
| Ta | 1 (0.2 %) | 24 (14.5 %) | 5 (5.4 %) | 110 (49.1 %) | 40 (30.8 %) | 0 (0 %) | 345 (72.5 %) |
| T1 | 3 (0.7 %) | 80 (48.5 %) | 10 (10.8 %) | 63 (28.1 %) | 51 (39.2 %) | 0 (0 %) | 112 (23.5 %) |
| T2-4 | 0 (0 %) | 0 (0 %) | 0 (0 %) | 0 (0 %) | 0 (0 %) | 0 (0 %) | 16 (3.4 %) |
| T2 | 117 (29.0 %) | 31 (18.8 %) | 17 (18.3 %) | 43 (19.2 %) | 38 (29.2 %) | 40 (63.5 %) | 0 (0 %) |
| T3 | 192 (47.6 %) | 19 (11.5 %) | 42 (45.2 %) | 7 (3.1 %) | 0 (0 %) | 16 (25.4 %) | 0 (0 %) |
| T4 | 57 (14.1 %) | 11 (6.7 %) | 19 (20.4 %) | 1 (0.4 %) | 0 (0 %) | 6 (9.5 %) | 0 (0 %) |
| unknown | 33 (8.2 %) | 0 (0 %) | 0 (0 %) | 0 (0 %) | 1 (0.8 %) | 0 (0 %) | 0 (0 %) |
| **Grade** | | | | | | | |
| High | 380 (94.3 %) | 60 (36.4 %) | 87 (93.5 %) | 0 (0 %) | 0 (0 %) | 0 (0 %) | 192 (40.3 %) |
| Low | 20 (5.0 %) | 105 (63.6 %) | 6 (6.5 %) | 0 (0 %) | 0 (0 %) | 0 (0 %) | 284 (59.7 %) |
| G1 | 0 (0 %) | 0 (0 %) | 0 (0 %) | 45 (20.1 %) | 15 (11.5 %) | 0 (0 %) | 0 (0 %) |
| G2 | 0 (0 %) | 0 (0 %) | 0 (0 %) | 84 (37.5 %) | 40 (30.8 %) | 0 (0 %) | 0 (0 %) |
| G3 | 0 (0 %) | 0 (0 %) | 0 (0 %) | 93 (41.5 %) | 75 (57.7 %) | 0 (0 %) | 0 (0 %) |
| unknown | 3 (0.7 %) | 0 (0 %) | 0 (0 %) | 2 (0.9 %) | 0 (0 %) | 63 (100 %) | 0 (0 %) |
| **Type** | | | | | | | |
| MIBC | 399 (99.0 %) | 62 (37.6 %) | 78 (83.9 %) | 51 (22.8 %) | 39 (30.0 %) | 62 (98.4 %) | 16 (3.4 %) |
| NMIBC | 4 (1.0 %) | 103 (62.4 %) | 15 (16.1 %) | 173 (77.2 %) | 91 (70.0 %) | 1 (1.6 %) | 460 (96.6 %) |

ous studies [47,48]. For these universally expressed proteins, the expression = the score of the positively stained region (0, negative expression; 1, 1–10 %; 2, 11–50 %; 3, 51–80 %; and 4, >80 %) × score of immunostaining intensity (0, negative staining; 1, weak staining; 2, mild staining; and 3, strong intensity) [49].

### 2.9. Statistical analysis

Kaplan–Meier plots and log-rank tests were performed to determine the survival difference between the BCIPI-H and BCIPI-L subgroups. In addition, multivariate Cox regression analysis was employed to synthesize the BCIPI and clinicopathological features and compare the predictive value of this newly established model with BCIPI versus that of a continuous C-index; subsequently, the restricted mean survival (RMS) curve was generated [50,51]. All analyses were performed using R software (version 3.6.5). A two-sided $P$ value < 0.05 was deemed statistically significant.

## 3. Results

### 3.1. Establishment and validation of the BCIPI signature

To comprehensively establish an immune component-based prognostic index in bladder cancer, we manually retrieved and modified 162 tumor-infiltrated immune signatures. The NES value of each signature in individuals was calculated by the ssGSEA method. Then, we employed univariate Cox regression analysis to determine the prognostic roles of these signatures in the four bladder cancer cohorts. meta-analyses were performed to achieve overall predictive estimations for the 162 immune-related signatures. As a result, 33 immune-related signatures with $P$ values $\leq$ 0.05 were enrolled in building the BCIPI, and the details of the signatures are illustrated in Supplementary Table 2 (all $P$ < 0.05).

The BCIPI score of each bladder cancer patient was calculated by adding the NES value of the 11 selected immune-related risk signatures and subtracting the NES score of 22 protect signatures, and a heatmap plot was employed to display the distributions of the 33 immune-related signatures between the BCIPI-H and BCIPI-L subgroups (Fig. 1A-B). The Kaplan–Meier plot suggested that the BCIPI was a risk factor for overall survival in all four bladder cancer cohorts (TCGA-BLCA: HR = 1.37, 95 % CI: 1.013–1.846, $P$ = 0.041, Fig. 1C; GSE13507: HR = 1.7, 95 % CI: 1.054–2.746, $P$ = 0.030, Fig. 1D; GSE31684: HR = 1.59, 95 % CI: 0.962–2.617, $P$ = 0.071, Fig. 1E; GSE32894: HR = 13.47, 95 % CI: 3.171–57.216, $P$ < 0.001, Fig. 1F), and the synthesized *meta*-analysis obtained more convincing results (HR = 1.84, 95 % CI: 1.15–2.95, $P$ = 0.010, Fig. 1G). In addition, we observed that BCIPI still presented a favorable prognostic value of over all survival (OS) for BCa patients, especially in the subgroup of G2 ($P$ = 0.001), G3 ($P$ = 0.005), and high grade ($P$ = 0.08) (Supplementary Fig. 1).

To further explore whether the BCIPI system could be included as a supplement to the currently available staging system, we employed RMS time ratios to compare patients' overall survival outcomes in different BCIPI subgroups. The RMS time ratios ranged from 0.65 to 0.84 in the four datasets (TCGA-BLCA: $P$ < 0.001; GSE13507: $P$ < 0.001; GSE31684: $P$ = 0.008; GSE32894: $P$ = 0.012, Fig. 2), and the overall predictive values were significantly improved in all four bladder cancer cohorts. These findings suggest that the newly defined BCIPI is an effective classification system that not only reflects the tumor immune infiltration status in the local bladder and predicts the overall survival of bladder cancer patients but also adds prognostic value to the available staging system.

### 3.2. Comparison of the tumor-infiltrated immunocytes between the BCIPI-H and BCIPI-L subgroups

GSEA was conducted to compare the BCIPI-H and BCIPI-L groups at the pathway level in the TCGA-BLCA cohort. As a result, we found that the differences between the two subgroups were significantly concentrated on immune-related pathways, including cell adhesion molecules cams, complement and coagulation cas-

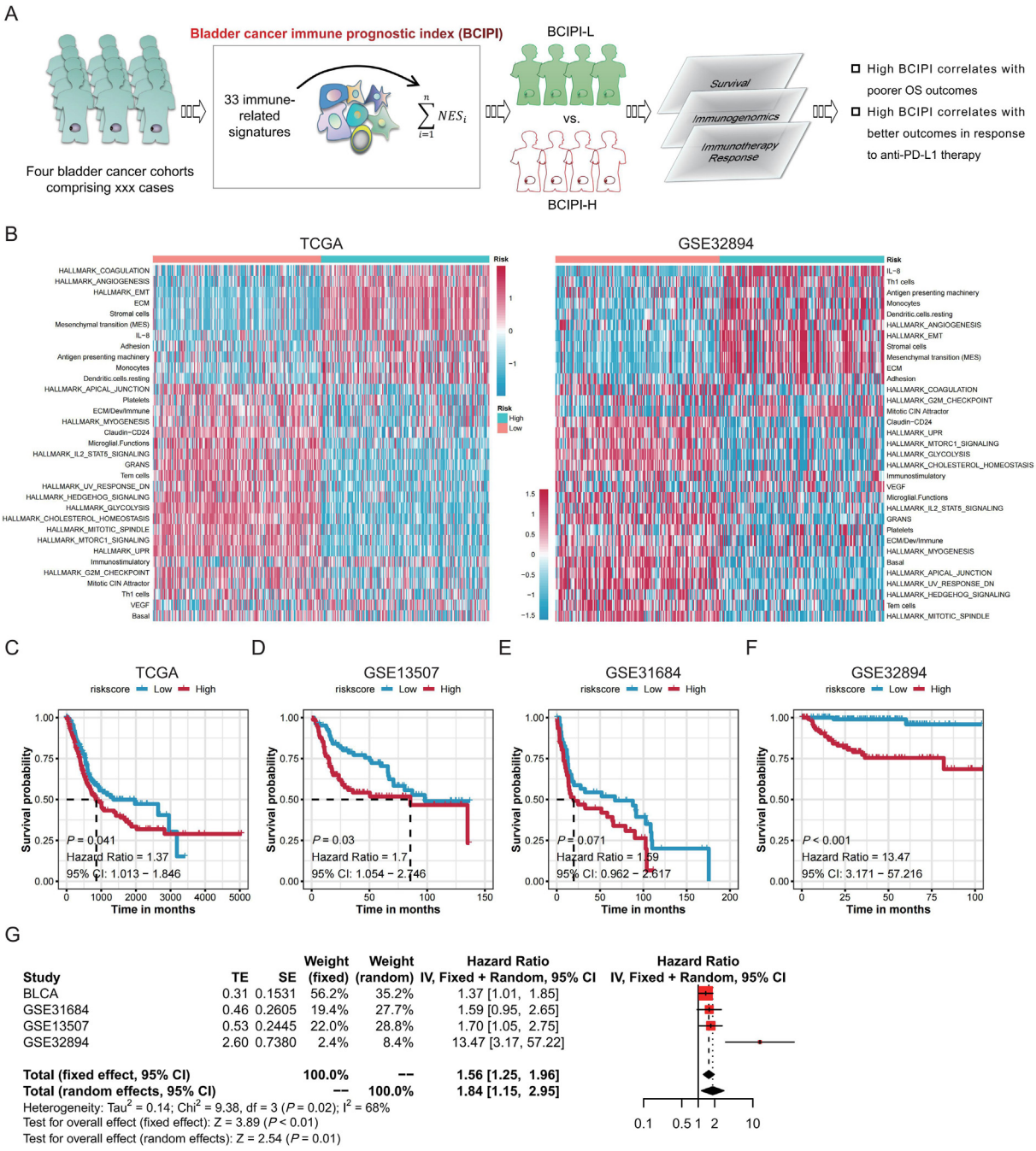


**Fig. 1.** The 33 immune-associated signatures-based indexes predict the overall survival of bladder cancer patients. (A) The flow displays the overall design of the current study. (B) Heatmaps displaying the normalized enrichment score (NES) between bladder cancer immune prognostic index (BCIPI)-high and -low subgroups in the TCGA-BLCA and GSE32894 cohorts. (C–F) Kaplan–Meier plot showing distinct overall survival outcomes between the BCIPI-high and BCIPI-low subgroups in the TCGA-BLCA, GSE13507, GSE31684, and GSE32894 cohorts. (G) Meta-analysis displaying the overall prognostic value of the BCIPI by synthesizing the hazard ratio (HR) values from four bladder cancer cohorts.

cades, cytokine receptor interaction, ECM receptor interaction, hematopoietic cell lineage, leukocyte transendothelial migration, neuroactive ligand receptor interaction, nod like receptor signaling pathway, pathways in cancer, and *T*-cell receptor signaling pathway ($P < 0.05$) (Fig. 3A, and Supplementary Table 3).

To assess whether the BCIPI reflects the tumor-infiltrated immunocytes/immune responses of bladder cancer patients, we evaluated the association between the BCIPI and ImmuneScore and TumourPurity, defined by Yoshihara et al. [40] as well as the StromalScore. The results depicted that the BCIPI was significantly positively associated with ImmuneScore and StromalScore, but negatively associated with TumourPurity. The details of the $\hat{R}_{Person}$ and *P* values in different data cohorts are displayed in Supplementary Fig. 2.

Moreover, we compared the infiltrating abundance of 28 immunocytes between the BCIPI-H and BCIPI-L groups in the four bladder cancer cohorts. As displayed in Fig. 3B, the abundance of nearly all immunocytes, such as activated B cells, activated $CD4^+$ T cells, macrophages, Th1 cells, and Tregs, among the four cohorts was higher in the BCIPI-H group than in the BCIPI-L group. We also validated these findings in bladder cancer tissue arrays (Supplementary Table 4). We chose CD163 as the marker of macrophages, and with the IHC staining results for CD163, we found that higher expression of CD163 was correlated with unfavorable prog-

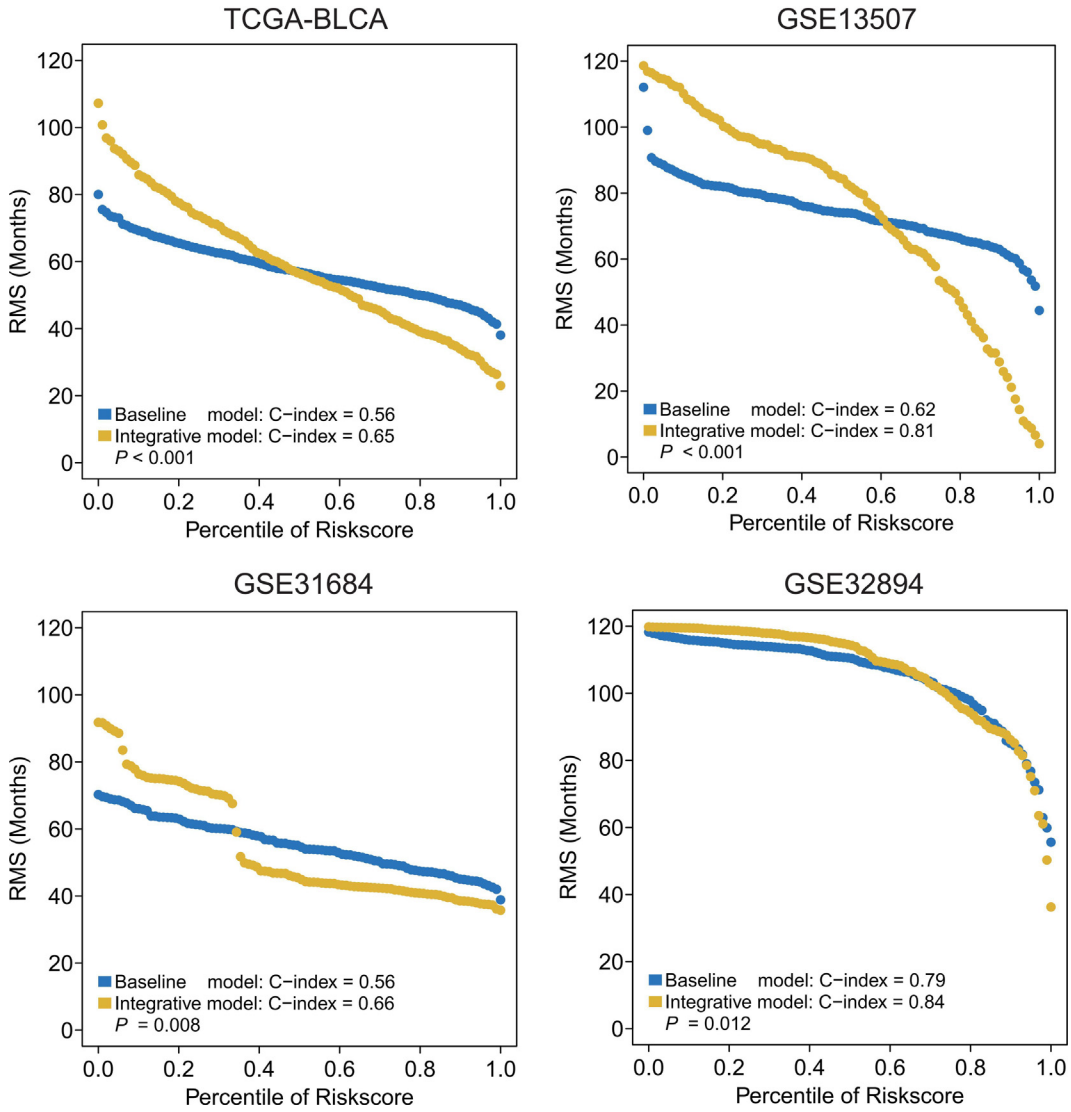


**Fig. 2.** Restricted mean survival (RMS) difference between the bladder cancer immune prognostic index (BCIPI) and the integrated signature in TCGA-BLCA, GSE13507, GSE31684, and GSE32894 cohorts. The integrated signature was generated by combining the BCIPI with clinicopathological features. The RMS curves are made up of a series of points representing the RMS time of matched BCIPI and integrated signature. The difference in terms of the C-index between the two signatures was determined by the *t*-test.

nosis in bladder cancer patients with a lower American Joint Committee on Cancer (AJCC) stage (Ois + I + II) (log-rank *P* value < 0.05, Fig. 3C–D), while a higher percentage of $CD8^+$ cells was correlated with favorable prognosis (log-rank *P* value < 0.05, Fig. 3E–F). No significant association was observed between PD-L1 expression and the overall survival of bladder cancer patients (Fig. 3G). In addition, the Pearson correlation test also suggested that the percentage of $CD8^+$ cells was significantly associated with overall survival (Pearson correlation test $P < 0.01$, Fig. 3H). Our results suggest that the BCIPI can reflect the immune status of bladder cancer patients, which might also be associated with the chemotherapy or immunotherapy response.

### 3.3. Patients in the BCIPI-H subgroup depicted a positive response to anti-PD-L1 treatment

As mentioned above, tumor immune status might be associated with immunotherapy response; thus, we assessed the correlation between the BCIPI and the expression of 66 immune checkpoints. We found that the BCIPI was significantly related to the expression of most immune checkpoints in the four cohorts (Supplementary Fig. 3). Notably, a positive association between PD-L1 and the BCIPI was identified in all four bladder cancer cohorts, and the mRNA expression of PD-L1 was higher in the BCIPI-H subgroup than in the BCIPI-L subgroup in these four cohorts (TCGA-BLCA: $P < 0.001$, Fig. 4A; GSE13507: $P = 0.0094$, Fig. 4C; GSE31684: $P = 0.00057$, Fig. 4E; GSE32894: $P < 0.001$, Fig. 4G). Subsequently, we assessed the association between BCIPI subgroups and anti-PD-L1 therapy response in these four bladder cancer cohorts, and the results suggested that patients in the BCIPI-H subgroup might benefit more from anti-PD-L1 therapy than those in the BCIPI-L subgroup (TCGA-BLCA, $P = 0.086$, Fig. 4B; GSE13507, $P = 0.019$, Fig. 4D; GSE31684, $P = 0.185$, Fig. 4F; GSE32894, $P = 0.007$, Fig. 4H). Our findings suggest that anti-PD-L1 therapy is a promising option for treating bladder cancer patients with a higher BCIPI.

### 3.4. Correlation of genomic alterations with the BCIPI subgroups in bladder cancer

Different populations carry different gene mutations [52], gene mutations might play important role in tumoregenisis and futher development [53]. We observed a significant mutational difference

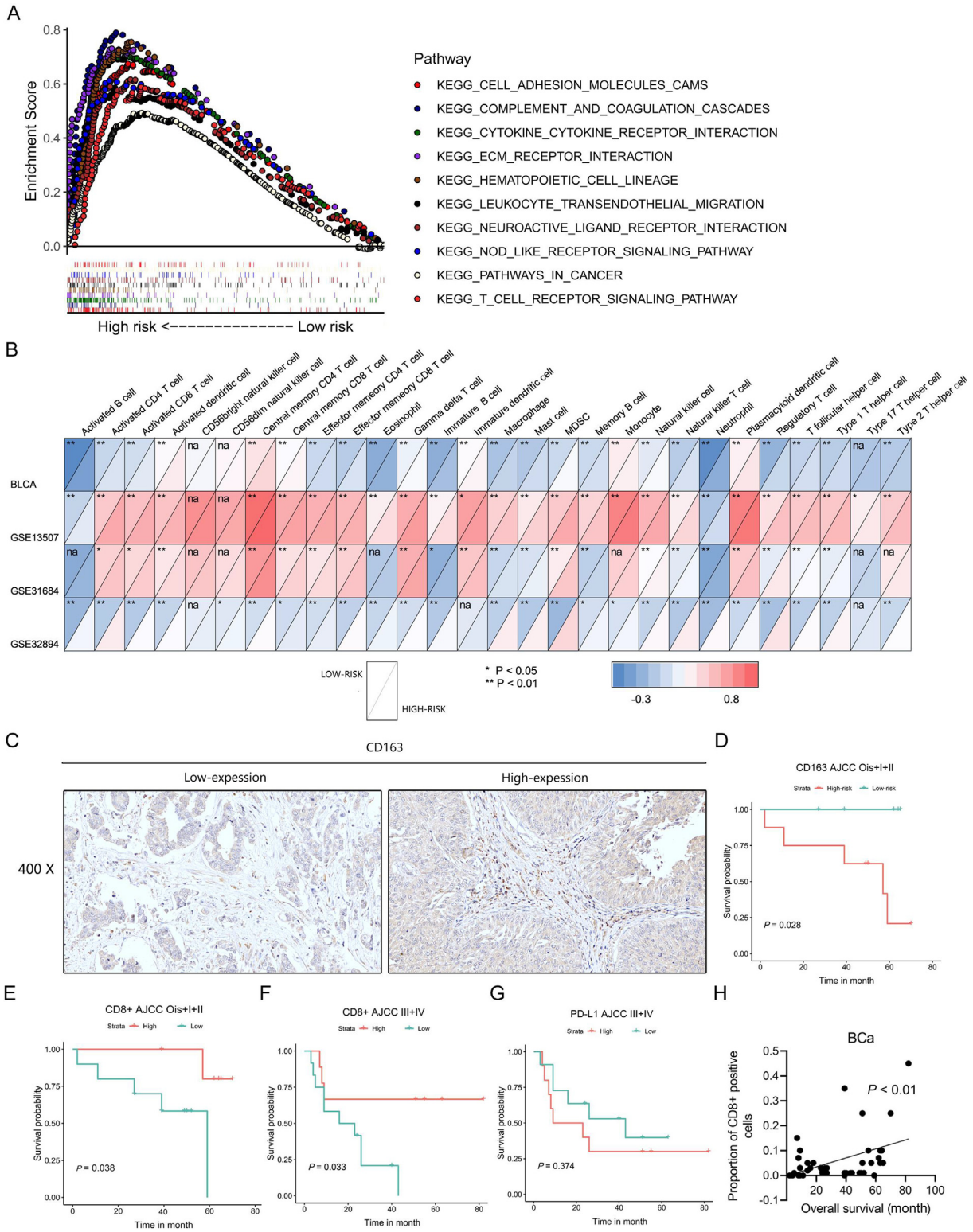


**Fig. 3.** The bladder cancer immune prognostic index (BCIPI)-high subgroup showed higher infiltration of immunocytes than the BCIPI-low subgroup. (A) Pathway enrichment differences between the bladder cancer immune prognostic index (BCIPI)-high and BCIPI-low subgroups revealed by Gene Set Enrichment Analysis (GSEA). (B) The infiltration difference of the 28 immunocytes between the BCIPI-High and BCIPI-Low subgroups in the TCGA-BLCA, GSE13507, GSE31684, and GSE32894 cohorts. (C–D) Kaplan–Meier and log-rank analyses revealed that higher expression of CD163 was significantly correlated with unfavorable prognosis of bladder cancer with early-stage disease (AJCC Ois + I + II). (E–F) Kaplan–Meier and log-rank analyses revealed that a higher percentage of $CD8^+$ positive cells was significantly correlated with a favorable prognosis for bladder cancer. (G) Kaplan–Meier and log-rank analyses revealed that a higher percentage of PD-L1-positive cells was seemingly associated with an unfavorable prognosis of bladder cancer. AJCC, American Joint Committee on Cancer.

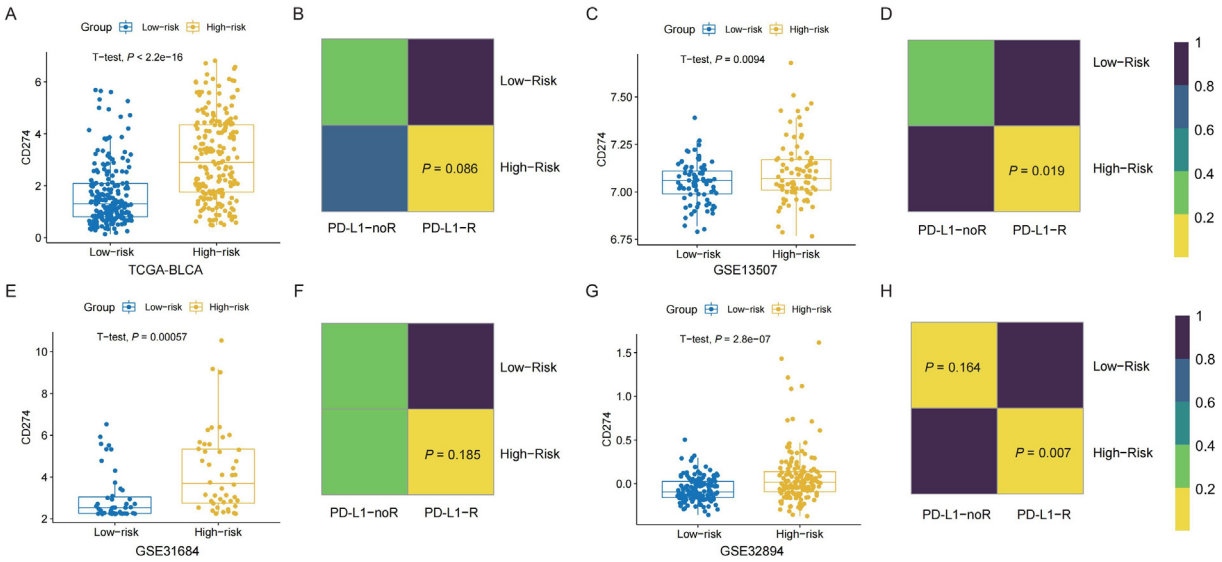


**Fig. 4.** The bladder cancer immune prognostic index (BCIPI) is associated with the response to anti-PD-L1 immunotherapy. CD274 (PD-L1) was more highly expressed in the BCIPI-High subgroup than in the BCIPI-Low subgroup in the TCGA-BLCA (A), GSE13507 (C), GSE31684 (E), and GSE32894 (G) cohorts. Patients in the BCIPI-High subgroup were predicted to have better anti-PD-L1 treatment effects in the TCGA-BLCA (B), GSE13507 (D), GSE31684 (F), and GSE32894 (H) cohorts.

between the BCIPI-L and BCIPI-H groups. KDM6A (33 % vs 19 %), FGFR3 (23 % vs 4 %), GRIA4 (7 % vs 1 %), CASC5 (8 % vs 1 %), ARHGAP35 (8 % vs 4 %), and SVEP1 (7 % vs 3 %) were significantly more highly mutated in the BCIPI-L group than in the BCIPI-H group (Fisher's exact P value < 0.05), while PHLDB2 (2 % vs 7 %), XIRP2 (8 % vs 16 %), INO80 (3 % vs 6 %), DSP (4 % vs 10 %), CUL9 (3 % vs 7 %), and AHNAK (7 % vs 12 %) were significantly more highly mutated in the BCIPI-H group than in the BCIPI-L group in the TCGA-BLCA cohort (Fisher's exact P value < 0.05) (Fig. 5A). We also found that patients in the BCIPI-H group displayed a lower level of CNV at the ArmDeletion level (*t*-test, PDeletion = 0.0097, Fig. 5B) but revealed a higher level of CNV at the FocalAmp level (*t*-test, PAmp = 0.012, Fig. 5C). We also analyzed the survival difference between altered (alterations occurred in the above genes) and unaltered (alterations have not occurred in the above genes) subgroups and found that the patients in the altered subgroup demonstrated better overall survival outcomes than those in the unaltered subgroup (log-rank *P* value = 0.033).

For these mutated genes, we focused on *FGFR3*, whose mutations resulted in higher expression of *FGFR3* (Fig. 5E). In addition, we analyzed the recurrent mutations in this gene between the BCIPI-H and BCIPI-L subgroups. We found that the mutation rates of the FGFR3-S249C allele were higher in the BCIPI-L group than in the BCIPI-H group (12.74 % vs 2.96 %), followed by G370C (2.45 % vs 0 %), and then Y373C (3.92 % vs 0 %) (Fig. 5F), indicating that these recurrent mutations might influence the expression of *FGFR3* and subsequently influence tumor microenvironment. These results suggested that *FGFR3* aberrations might be associated with tumor microenvironment in bladder cancer.

### *3.5. Validation of BCIPI in external cohorts and compare with proposed molecular subtypes*

The external cohorts, GSE32548, GSE48075, and E-MTAB-4321, were used to validate the prognostic value of BCIPI. The GSE32548 cohort contains 91 non-muscular invasive bladder cancer (NMIBC) cases and 39 muscular invasive bladder cancer (MIBC) cases; GSE48075 contains one NMIBC case and 62 MIBC cases; these two cohorts recorded the OS information. The E-MTAB-4321 cohort contains 476 NMIBC patients, with the available progression information recorded. After calculation of the BCIPI score, we observed that BCIPI presented excellent predictive value in the GSE32548 ($P$ < 0.001, HR = 5.31, 95 % CI: 1.986–14.187, Fig. 6A), GSE48075 ($P$ = 0.036, HR = 2.06, 95 % CI: 1.047–4.043, Fig. 6B), and E-MTAB-4321 ($P$ = 0.005, HR = 3.21, 95 % CI: 1.435–7.173, Fig. 6C) cohorts.

In addition, we also compared the BCIPI risk subgroups with several proposed molecular classifiers. The TCGA group proposed a new molecular classification system in bladder cancer that includes five molecular subtypes (luminal, luminal-papillary/infiltrated, basal/squamous, and neuronal [45]); we identified that the patients in the BCIPI-H group were mainly attributed to the basal squamous and luminal-infiltrated subtypes, while the patients in the BCIPI-L group were mapped to the luminal-papillary and luminal subtypes (Fig. 6D), which was consistent with the survival analyses that demonstrated that patients with the basal squamous and luminal-infiltrated subtypes had a more unfavorable prognosis than those with the luminal-papillary and luminal subtypes (log-rank *P* value = 0.002, Fig. 6D). Kamoun et al. [54] reported a consensus bladder cancer molecular subtype, and we compared BCIPI with it in the TCGA-BLCA cohort. We found that BCIPI-H patients accounted for most parts of the Ba/Sq type and stroma-rich type, which also had poor prognosis, while BCIPI-L patients were mostly from the favorable prognosis LumP type (Fig. 6E). An unusual situation is that although the NE-like subtype has the worst prognosis, it is classified as BCIPI-L in our grouping, which reflects that the prognosis of the NE-like subtype is not related to the activation of immune pathways. For NMIBC, Hedegaard et al. [55] demonstrated a molecular subtype based on the E-MTAB-4321 cohort, including basal-like, CIS-like, and luminal subtypes, with the CIS-like subtype having the worst progression survival and the luminal subtype having the most favorable clinical outcome. We compared BCIPI with Hedegaard subtypes and observed that BCIPI-H was similar to the CIS-like subtype, while BCIPI-L was mostly composed of the luminal and basal-like subtypes (Fig. 6F). Furthermore, we combined the BCIPI risk subgroups with the above molecular classifiers to analyse the prognosis of patients in different subgroups. For MIBC in the TCGA subtype, we found that patients with the luminal infiltrated subtype with high immune activation had a more unfavorable prognosis, while low immune activation indicated a better prognosis. For

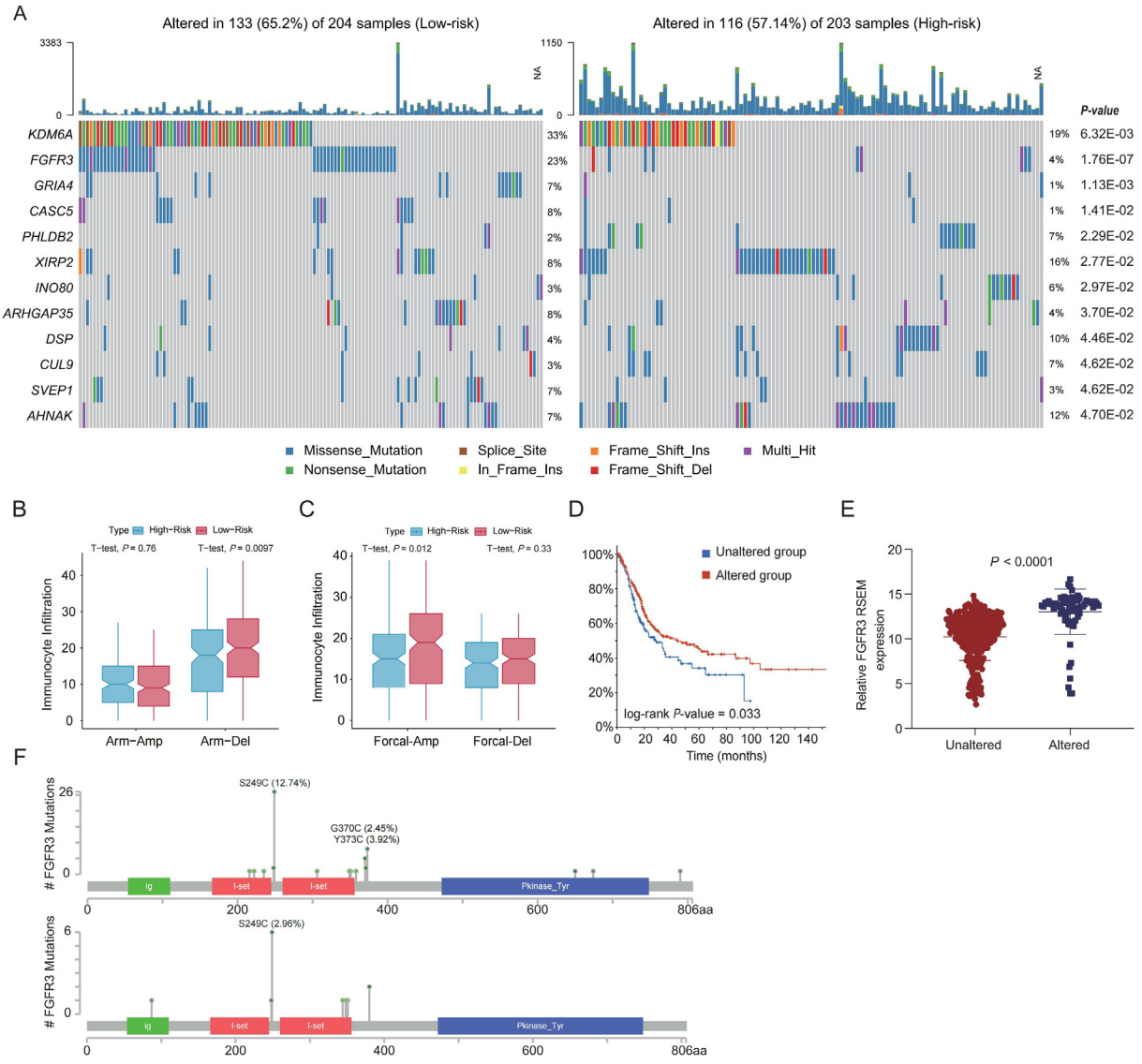


**Fig. 5.** Genetic differences between the bladder cancer immune prognostic index (BCIPI)-high and BCIPI-low subgroups. (A) Oncoprint plot displaying the significantly differentially mutated genes between BCIPI-High and BCIPI-Low subgroups. (B–C) The distribution difference in Arm- (B) and Focal-level (C) copy number variations (CNVs), including amplification (Amp) and deletion (Del). (D) Kaplan–Meier plot and log-rank analyses displaying the survival difference between gene-altered (patients with mutations of significantly differentially mutated genes) and unaltered (patients without mutations of significantly differentially mutated genes) subgroups in the TCGA-BLCA cohort. (E) FGFR expression was more highly expressed in gene-altered (patients with mutations of significantly differentially mutated genes) than unaltered (patients without mutations of significantly differentially mutated genes) subgroups in the TCGA-BLCA cohort. (F) The lollipop plot displays the major mutated sites of FGFR in the BCIPH-High (down) and BCIPI-Low (up) groups.

patients with the neuronal subtype, high immune activation indicated a better prognosis than those with low immune activation. However, other molecular subtypes did not present different survival prognoses impacted by the different immune activation (Supplementary Fig. 4A). In the Kamoun consensus subtype, we found that patients with LumU and Stroma-rich subtypes with high immune activation had a better prognosis than those with low immune activation. For patients with the LumP subtype, high immune activation indicated a more unfavorable prognosis than low immune activation (Supplementary Fig. 4B). For NMIBC in the Hedegaard subtype, patients with basal-like and luminal subtypes with high immune activation had a more unfavorable prognosis than those with low immune activation (Supplementary Fig. 4C). These results also confirm the prognostic value of BCIPI in both MIBC and NMIBC.

## 4. Discussion

Immune components play critical roles in bladder cancer. Here, we constructed a prognostic index based on the essential infiltrated immunocyte/tumor immune responses. We found that the BCIPI successfully discriminated low- and high-risk patients with distinct overall survival outcomes. In addition, significant differences between the BCIPI subgroups and CNVs, somatic mutations, immunomodulators, and infiltrated immunocyte abundance were identified. Notably, we also found that patients in the BCIPI-H subgroup might be more sensitive in response to anti-PD-L1 immunotherapy. Our findings will help clinicians to develop individualized treatment plans.

Most of the current research on immunotherapy biomarkers concentrates on a single gene or different tumor-infiltrating

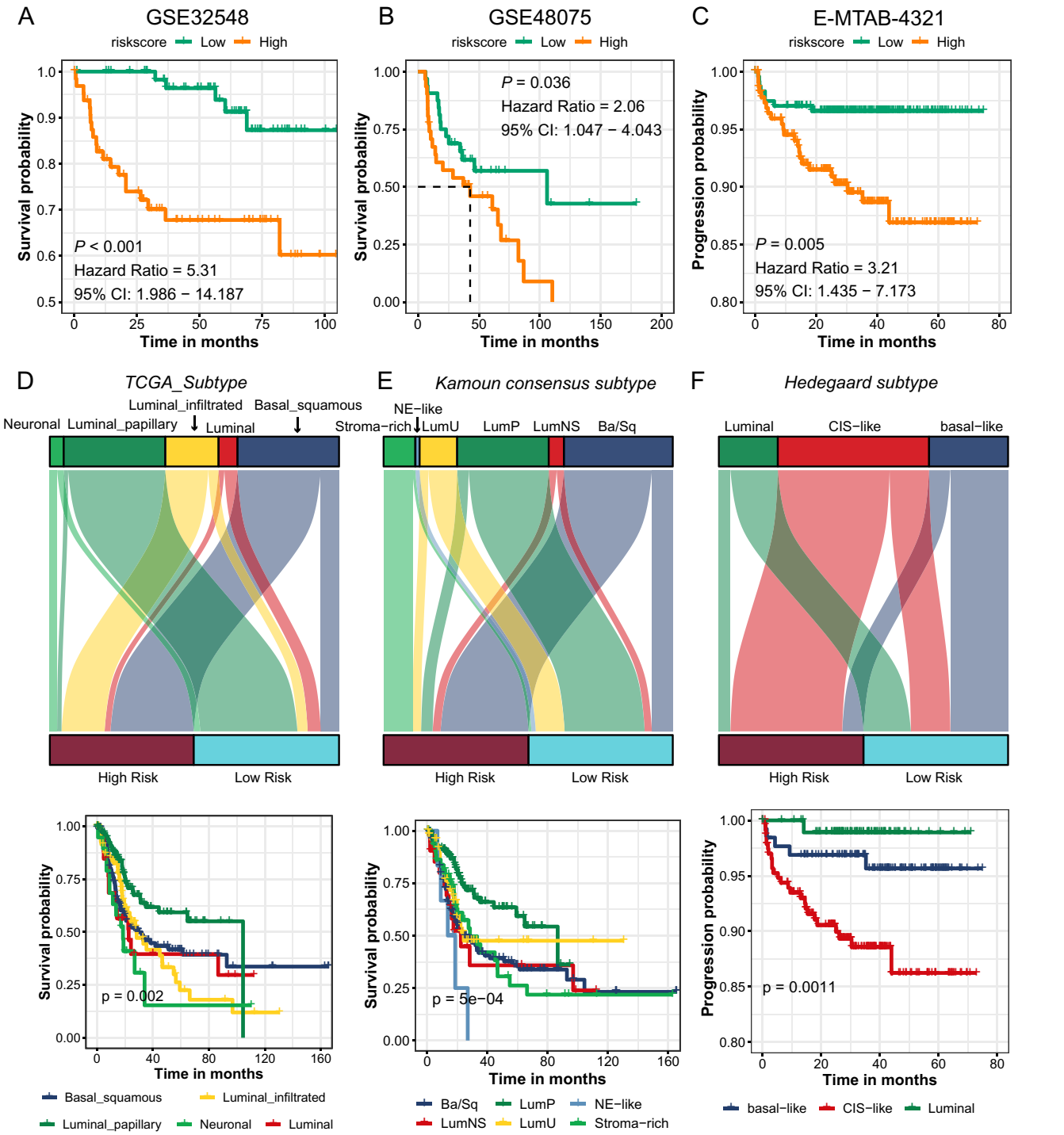


**Fig. 6.** Validation of bladder cancer immune prognostic index (BCIPI) in external cohort and comparison with proposed molecular subtypes. (A) Kaplan–Meier plot showing the prognostic value of BCIPI for overall survival in GSE32584. (B) Kaplan–Meier plot showing the prognostic value of BCIPI to overall survival in GSE48075. (C) Kaplan–Meier plot showing the prognostic value of BCIPI for tumor progression in E-MTAB-4321. (D) Sankey plot displaying the correlation between BCIPI subgroups and TCGA-BLCA molecular subgroups; Kaplan–Meier plot showing the distinct survival outcome of basal squamous, luminal, luminal-infiltrated, luminal-papillary, and neuronal subtypes. (E) Sankey plot displaying the correlation between BCIPI subgroups and Kamoun et al.'s consensus subtype, Kaplan–Meier plot showing the distinct survival outcome of stroma-rich, NE-like, LumU, LumP, LumNS, and Ba/Bq subtypes. (F) Sankey plot displaying the correlation between BCIPI subgroups and Hedegaard et al.'s consensus subtype; Kaplan–Meier plot showing the distinct survival outcome of Luminal, CIS-like, and basal-like subtypes.

lymphocytes ratios. These may be insufficient predictors of patient response to immunotherapy. Compared to most of the biomarkers currently used, the BCIPI is more comprehensive in considering the immune signatures. We manually retrieved and modified 162 tumor-infiltrated immune signatures. After a series of analyses, 33 immune-related signatures were enrolled in building the BCIPI. After that, we wanted to identify the correspondence between the BCIPI and immune therapy, so we analyzed the BCIPI in four cohorts (TCGA-BLCA, GSE13507, GSE31684, and GSE32894) and found that patients in the BCIPI-H subgroup revealed a positive response to anti-PD-L1 treatment. As for the prognostic predictive value of the BCIPI, we analyzed the BCIPI in the four cohorts and

then validated it in three external cohorts (GSE32548, GSE48075, and E-MTAB-4321), then compared it with proposed molecular subtypes. We compared the difference of tumor-infiltrated immunocytes and genomic alterations between the BCIPI-H and BCIPI-L subgroup. The differences of pathways and genes may reflect the potential prognostic predictive mechanisms of the BCIPI. We found that the BCIPI could predict the overall survival of bladder cancer patients and add prognostic value to the available staging system. The BCIPI is a special and effective classification system that can not only predict the response to immunotherapy but also has prognostic predictive value for patients with bladder cancer.

Previous studies have reported that higher infiltration of immunocytes is correlated with a favorable prognosis for bladder cancer [55], while many studies have indicated that denser tumor-infiltrating lymphocytes are associated with more invasive features [56,57]. Commonly, lymphocytes migrate to the tumor site from the circulating immune system, indicating that the host immune system can initiate an antitumor response. However, the immunosuppressive microenvironment is created after tumor cells acquire genetic aberrations, and this kind of variation blocks tumor clearance by the infiltrated immunocytes. In that case, the predictive value of tumor-infiltrated immunocytes would be limited. Here, we comprehensively retrieved immune-related signatures, and based on a series of analyses; we established an infiltrated immunocyte/immune response-based index. We found that this index reflects the type and activity of these infiltrated immune components and can predict the overall survival of bladder cancer patients. Although we found that immune status was associated with prognosis, the prognostic predictive value of the BCIPI was affected by the proposed molecular classifiers. We found that for MIBC in the TCGA subtype and Kamoun consensus subtype, patients with the luminal infiltrated subtype, neuronal subtype, LumU, and stroma-rich and LumP subtypes, the different immune activation might indicate different prognoses. For NMIBC in the Hedegaard subtype, patients with basal-like and luminal subtypes with high immune activation had a more unfavorable prognosis than those with low immune activation. Subsequent studies are warranted to validate our findings and to reveal the underlying mechanisms behind them.

For these differentially mutated genes, we are interested in FGFR3. As indicated in previous studies, FGFR3 mutations are commonly correlated with low-grade and stage of bladder cancer [58], as well as common disease-specific progression [58–60]. Nevertheless, based on FGFR3 mutations being associated with favorable features in bladder cancer, there is a lack of evidence to propose that FGFR3 mutations are linked to less aggressive characteristics. In addition, for bladder cancer patients at an advanced stage or who are receiving chemotherapy, FGFR3 mutations are associated with unfavorable outcomes [45,61]. The proper application of FGFR3 inhibition in the context of immune checkpoint inhibitor (ICI) therapy has been clinically investigated at an early stage. It has been reported that patients who had received ICI therapy demonstrated higher response rates to FGFR inhibition than the cohort (59 % vs 40 %) [62,63]. Rogaratinib also obtained a similar effect of 30 % response among patients treated with ICI compared with 24 % across the overall cohort [64]. The reasons for this phenomenon include FGFR inhibition altering the microenvironment and tumor cells being "sensitized" to allow for lymphocyte invasion. In addition, FGFR signaling might be activated during tumor progression or immunotherapy resistance. More studies are needed to investigate the interaction between FGFR3 mutation and tumor microenvironment formation or immunotherapy response.

Recently, immunotherapeutic agents, such as PD-1 and PD-L1, have provided novel treatment options for patients with metastatic bladder cancer [7]. In addition, these drugs have been proven to be associated with prolonged stable responses in these patients [6]. Increasing evidence suggests that tumor-infiltrated immunocytes, tumor mutational burden, copy number variations, and the number of neoantigens are correlated with the immunotherapeutic response [7–10]. Our study found that the BCIPI-H subgroup is predicted to be more sensitive in response to anti-PD-L1 immunotherapy. Consistently, the expression of CD274 was also higher in the BCIPI-H subgroup than in the BCIPI-L subgroup. Bladder cancer patients with higher PD-L1 expression tend to have progressive cancer and unfavorable prognoses [65,66]. Furthermore, Rosenberg et al. [67] found that the antitumor response to atezolizumab (anti-PD-L1) relied on the PD-L1 expression level in tumor-infiltrating immunocytes. Combining the data from the literature and our findings, we conclude that although patients in the BCIPI-H subgroup have mostly unfavorable prognoses, they tend to be more sensitive to anti-PD-L1 immunotherapy when metastases occur because of the higher abundance of infiltrated immunocytes and higher activity of immune responses than the BCIPI-L subgroup.

We summarize three advantages of the BCIPI. First, we comprehensively retrieved immunocyte/immune response-related signatures. We established an effective classification system with a series of analyses and proved the usage and stability of this index in four independent cohorts comprising 888 bladder cancer cases. Second, based on the correlation between tumor-infiltrated immunocytes/immune responses and response to immunotherapy, we performed systematic analyses and predicted that patients in the BCIPI-H subgroup are more sensitive in response to anti-PD-L1 therapy, which offers inspiration for clinical treatment. Third, we observed significant differences between the BCIPI-H and BCIPI-L subgroups in pathway enrichment, mutated genes, CNVs, and tumor-infiltrated immunocytes/immune responses. These findings will guide the design of future mechanism studies. There are also several limitations of the current work. First, although we predicted the anti-PD-L1 immunotherapy responses of the four bladder cancer cohorts based on a public dataset including bladder cancer patients after receiving immunotherapy, we still need to validate our findings in an external bladder cancer cohort that will receive or has already received anti-PD-L1 immunotherapy. Second, we observed significant differences at the multiomics level within BCIPI subgroups, but future studies are warranted to reveal the underlying mechanisms behind them.

## 5. Conclusions

The correlation of the BCIPI with tumor-infiltrated immunocytes/immune responses, overall survival outcomes, and anti-PD-L1 immunotherapy indicates that this index is a robust classification system in bladder cancer. Patients in the BCIPI-H subgroup are associated with unfavorable prognoses but are presumed to have better treatment outcomes with anti-PD-L1 immunotherapy. These findings will help clinicians facilitate personalized treatment for bladder cancer patients.

## Ethics approval and consent to participate

The research contents and research programs were reviewed and approved by the Ethics Committee of the First Affiliated Hospital of Anhui Medical University (PJ2021-08-30).

## Consent for publication

Not applicable.

## Availability of data and materials

All data used in the current work can be downloaded from the GDC portal (https://portal.gdc.cancer.gov/), Gene-Expression Omnibus (GEO; https://www.ncbi.nlm.nih.gov/geo/) databases and https://www.ebi.ac.uk/biostudies/arrayexpress/studies/E-MTAB-4321.

## Author statement

MZ, JM, and CL designed the study; ZB, CL, and JC collected the data; MZ, JM, and QG analysed and interpretated the data. JM, MZ and ZB wrote the manuscript; All authors read and approved the final manuscript.

## Declaration of Competing Interest

The authors declare that they have no known competing financial interests or personal relationships that could have appeared to influence the work reported in this paper.

## Acknowledgements

The National Natural Science Foundation of China 81802827. Scientific Research Foundation of the Institute for Translational Medicine of Anhui Province (2017ZHYX02). The Natural Science Foundation of Guangdong Province, China (2017A030313800). Scientific Research Funding of Anhui Medical University (2020xkj157).

## Appendix A. Supplementary data

Supplementary data to this article can be found online at https://doi.org/10.1016/j.csbj.2022.11.052.

## References

[1] Siegel RL, Miller KD, Fuchs HE, Jemal A. Cancer Statistics, 2021. CA: A Cancer Journal for Clinicians. 2021;71(1):7-33.
[2] von der Maase H, Sengelov L, Roberts JT, Ricci S, Dogliotti L, Oliver T, et al. Long-term survival results of a randomized trial comparing gemcitabine plus cisplatin, with methotrexate, vinblastine, doxorubicin, plus cisplatin in patients with bladder cancer. J Clin Oncol 2005;23(21):4602–8.
[3] Altorki NK, Markowitz GJ, Gao D, Port JL, Saxena A, Stiles B, et al. The lung microenvironment: an important regulator of tumour growth and metastasis. Nat Rev Cancer 2019;19(1):9–31.
[4] Sharma P, Shen Y, Wen S, Yamada S, Jungbluth AA, Gnjatic S, et al. CD8 tumor-infiltrating lymphocytes are predictive of survival in muscle-invasive urothelial carcinoma. Proc Natl Acad Sci U S A 2007;104(10):3967–72.
[5] Pichler R, Fritz J, Zavadil C, Schäfer G, Culig Z, Brunner A. Tumor-infiltrating immune cell subpopulations influence the oncologic outcome after intravesical Bacillus Calmette-Guérin therapy in bladder cancer. Oncotarget 2016;7(26):39916–30.
[6] Bellmunt J, Powles T, Vogelzang NJ. A review on the evolution of PD-1/PD-L1 immunotherapy for bladder cancer: The future is now. Cancer Treat Rev 2017;54:58–67.
[7] Mariathasan S, Turley SJ, Nickles D, Castiglioni A, Yuen K, Wang Y, et al. TGFβ attenuates tumour response to PD-L1 blockade by contributing to exclusion of T cells. Nature 2018;554(7693):544–8.
[8] Topalian SL, Drake CG, Pardoll DM. Immune checkpoint blockade: a common denominator approach to cancer therapy. Cancer Cell 2015;27(4):450–61.
[9] Schumacher TN, Schreiber RD. Neoantigens in cancer immunotherapy. Science 2015;348(6230):69–74.
[10] Dieu-Nosjean MC, Antoine M, Danel C, Heudes D, Wislez M, Poulot V, et al. Long-term survival for patients with non-small-cell lung cancer with intratumoral lymphoid structures. J Clin Oncol 2008;26(27):4410–7.
[11] Gautier L, Cope L, Bolstad BM, Irizarry RA. affy–analysis of Affymetrix GeneChip data at the probe level. Bioinformatics (Oxford, England) 2004;20(3):307–15.
[12] Cheng WY, Ou Yang TH, Anastassiou D. Biomolecular events in cancer revealed by attractor metagenes. PLoS Comput Biol 2013;9(2):e1002920.
[13] Senbabaoglu Y, Gejman RS, Winer AG, Liu M, Van Allen EM, de Velasco G, et al. Tumor immune microenvironment characterization in clear cell renal cell carcinoma identifies prognostic and immunotherapeutically relevant messenger RNA signatures. Genome Biol 2016;17(1):231.
[14] Wolf DM, Lenburg ME, Yau C, Boudreau A, van 't Veer LJ. Gene co-expression modules as clinically relevant hallmarks of breast cancer diversity. PLoS One. 2014;9(2):e88309.
[15] Cheng WY, Ou Yang TH, Anastassiou D. Development of a prognostic model for breast cancer survival in an open challenge environment. Sci Transl Med 2013;5(181):181ra50.
[16] Bindea G, Mlecnik B, Tosolini M, Kirilovsky A, Waldner M, Obenauf AC, et al. Spatiotemporal dynamics of intratumoral immune cells reveal the immune landscape in human cancer. Immunity 2013;39(4):782–95.
[17] Newman AM, Liu CL, Green MR, Gentles AJ, Feng W, Xu Y, et al. Robust enumeration of cell subsets from tissue expression profiles. Nat Methods 2015;12(5):453–7.
[18] Fan C, Prat A, Parker JS, Liu Y, Carey LA, Troester MA, et al. Building prognostic models for breast cancer patients using clinical variables and hundreds of gene expression signatures. BMC Med Genomics 2011;4:3.
[19] Palmer C, Diehn M, Alizadeh AA, Brown PO. Cell-type specific gene expression profiles of leukocytes in human peripheral blood. BMC Genomics 2006;7:115.
[20] Iglesia MD, Vincent BG, Parker JS, Hoadley KA, Carey LA, Perou CM, et al. Prognostic B-cell signatures using mRNA-seq in patients with subtype-specific breast and ovarian cancer. Clin Cancer Res 2014;20(14):3818–29.
[21] Schmidt M, Bohm D, von Torne C, Steiner E, Puhl A, Pilch H, et al. The humoral immune system has a key prognostic impact in node-negative breast cancer. Cancer Res 2008;68(13):5405–13.
[22] Rody A, Karn T, Liedtke C, Pusztai L, Ruckhaeberle E, Hanker L, et al. A clinically relevant gene signature in triple negative and basal-like breast cancer. Breast Cancer Res 2011;13(5):R97.
[23] Rody A, Holtrich U, Pusztai L, Liedtke C, Gaetje R, Ruckhaeberle E, et al. T-cell metagene predicts a favorable prognosis in estrogen receptor-negative and HER2-positive breast cancers. Breast Cancer Res 2009;11(2):R15.
[24] Beck AH, Espinosa I, Edris B, Li R, Montgomery K, Zhu S, et al. The macrophage colony-stimulating factor 1 response signature in breast carcinoma. Clin Cancer Res 2009;15(3):778–87.
[25] Bedognetti D, Hendrickx W, Ceccarelli M, Miller LD, Seliger B. Disentangling the relationship between tumor genetic programs and immune responsiveness. Curr Opin Immunol 2016;39:150–8.
[26] Galon J, Angell HK, Bedognetti D, Marincola FM. The continuum of cancer immunosurveillance: prognostic, predictive, and mechanistic signatures. Immunity 2013;39(1):11–26.
[27] Hendrickx W, Simeone I, Anjum S, Mokrab Y, Bertucci F, Finetti P, et al. Identification of genetic determinants of breast cancer immune phenotypes by integrative genome-scale analysis. Oncoimmunology 2017;6(2):e1253654.
[28] Hu W, Wang Y, Fang Z, He W, Li S. Integrated characterization of lncRNA-immune interactions in prostate cancer. Front Cell Dev Biol 2021;9:641891.
[29] Papanicolau-Sengos A, Yang Y, Pabla S, Lenzo FL, Kato S, Kurzrock R, et al. Identification of targets for prostate cancer immunotherapy. Prostate 2019;79(5):498–505.
[30] Zhao SG, Lehrer J, Chang SL, Das R, Erho N, Liu Y, et al. The immune landscape of prostate cancer and nomination of PD-L2 as a potential therapeutic target. J Natl Cancer Inst 2019;111(3):301–10.
[31] Nair SS, Weil R, Dovey Z, Davis A, Tewari AK. The tumor microenvironment and immunotherapy in prostate and bladder cancer. Urol Clin North Am 2020;47(4s):e17–54.
[32] Song J, Chen W, Zhu G, Wang W, Sun F, Zhu J. Immunogenomic profiling and classification of prostate cancer based on HIF-1 signaling pathway. Front Oncol 2020;10:1374.
[33] Nirmal AJ, Regan T, Shih BB, Hume DA, Sims AH, Freeman TC. Immune cell gene signatures for profiling the microenvironment of solid tumors. Cancer Immunol Res 2018;6(11):1388–400.
[34] Chen B, Khodadoust MS, Liu CL, Newman AM, Alizadeh AA. Profiling tumor infiltrating immune cells with CIBERSORT. Methods Mol Biol 2018;1711:243–59.
[35] Wang L, Saci A, Szabo PM, Chasalow SD, Castillo-Martin M, Domingo-Domenech J, et al. EMT- and stroma-related gene expression and resistance to PD-1 blockade in urothelial cancer. Nat Commun 2018;9(1):3503.
[36] Efstathiou JA, Mouw KW, Gibb EA, Liu Y, Wu C-L, Drumm MR, et al. Impact of Immune and stromal infiltration on outcomes following bladder-sparing trimodality therapy for muscle-invasive bladder cancer. Eur Urol 2019;76(1):59–68.
[37] Yu G, Wang LG, Han Y, He QY. clusterProfiler: an R package for comparing biological themes among gene clusters. OMICS 2012;16(5):284–7.
[38] Hanzelmann S, Castelo R, Guinney J. GSVA: gene set variation analysis for microarray and RNA-seq data. BMC Bioinf 2013;14:7.
[39] Barbie DA, Tamayo P, Boehm JS, Kim SY, Moody SE, Dunn IF, et al. Systematic RNA interference reveals that oncogenic KRAS-driven cancers require TBK1. Nature 2009;462(7269):108–12.
[40] Yoshihara K, Shahmoradgoli M, Martinez E, Vegesna R, Kim H, Torres-Garcia W, et al. Inferring tumour purity and stromal and immune cell admixture from expression data. Nat Commun 2013;4:2612.
[41] Charoentong P, Finotello F, Angelova M, Mayer C, Efremova M, Rieder D, et al. Pan-cancer immunogenomic analyses reveal genotype-immunophenotype relationships and predictors of response to checkpoint blockade. Cell Rep 2017;18(1):248–62.
[42] Hoshida Y, Brunet JP, Tamayo P, Golub TR, Mesirov JP. Subclass mapping: identifying common subtypes in independent disease data sets. PLoS One 2007;2(11):e1195.

[43] Colaprico A, Silva TC, Olsen C, Garofano L, Cava C, Garolini D, et al. TCGAbiolinks: an R/Bioconductor package for integrative analysis of TCGA data. Nucleic Acids Res 2016;44(8):e71.
[44] Mayakonda A, Lin DC, Assenov Y, Plass C, Koeffler HP. Maftools: efficient and comprehensive analysis of somatic variants in cancer. Genome Res 2018;28(11):1747–56.
[45] Robertson AG, Kim J, Al-Ahmadie H, Bellmunt J, Guo G, Cherniack AD, et al. Comprehensive molecular characterization of muscle-invasive bladder cancer. Cell 2018;174(4):1033.
[46] Thorsson V, Gibbs DL, Brown SD, Wolf D, Bortone DS, Ou Yang TH, et al. The immune landscape of cancer. Immunity 2018.
[47] Yin Y, Xu L, Chang Y, Zeng T, Chen X, Wang A, et al. N-Myc promotes therapeutic resistance development of neuroendocrine prostate cancer by differentially regulating miR-421/ATM pathway. Mol Cancer 2019;18(1):11.
[48] Chen J, Zhan C, Zhang L, Zhang L, Liu Y, Zhang Y, et al. The hypermethylation of Foxp3 promoter impairs the function of Treg cells in EAP. Inflammation 2019;42(5):1705–18.
[49] Schneider CA, Rasband WS, Eliceiri KW. NIH image to ImageJ: 25 years of image analysis. Nat Methods 2012;9(7):671–5.
[50] Eng KH, Schiller E, Morrell K. On representing the prognostic value of continuous gene expression biomarkers with the restricted mean survival curve. Oncotarget 2015;6(34):36308–18.
[51] Uno H, Claggett B, Tian L, Inoue E, Gallo P, Miyata T, et al. Moving beyond the hazard ratio in quantifying the between-group difference in survival analysis. J Clin Oncol 2014;32(22):2380–5.
[52] Kessler MD, Loesch DP, Perry JA, Heard-Costa NL, Taliun D, Cade BE, et al. De novo mutations across 1,465 diverse genomes reveal mutational insights and reductions in the Amish founder population. Proc Natl Acad Sci U S A. 2020;117(5):2560-9.
[53] Mu R, Liu H, Luo S, Patz Jr EF, Glass C, Su L, et al. Genetic variants of CHEK1, PRIM2 and CDK6 in the mitotic phase-related pathway are associated with nonsmall cell lung cancer survival. Int J Cancer 2021;149(6):1302–12.
[54] Kamoun A, de Reynies A, Allory Y, Sjodahl G, Robertson AG, Seiler R, et al. A consensus molecular classification of muscle-invasive bladder cancer. Eur Urol 2020;77(4):420–33.
[55] Hedegaard J, Lamy P, Nordentoft I, Algaba F, Hoyer S, Ulhoi BP, et al. Comprehensive transcriptional analysis of early-stage urothelial carcinoma. Cancer Cell 2016;30(1):27–42.
[56] Morita T, Tokue A, Minato N. Analysis of natural killer activity and natural killer cell subsets in patients with bladder cancer. Cancer Immunol Immunother 1990;32(3):191–4.
[57] Ikemoto S, Kishimoto T, Wada S, Nishio S, Maekawa M. Clinical studies on cell-mediated immunity in patients with urinary bladder carcinoma: blastogenic response, interleukin-2 production and interferon-gamma production of lymphocytes. Br J Urol 1990;65(4):333–8.
[58] Pietzak EJ, Bagrodia A, Cha EK, Drill EN, Iyer G, Isharwal S, et al. Next-generation sequencing of nonmuscle invasive bladder cancer reveals potential biomarkers and rational therapeutic targets. Eur Urol 2017;72(6):952–9.
[59] Akanksha M, Sandhya S. Role of FGFR3 in urothelial carcinoma. Iran J Pathol 2019;14(2):148–55.
[60] van Rhijn BWG, Mertens LS, Mayr R, Bostrom PJ, Real FX, Zwarthoff EC, et al. FGFR3 mutation status and FGFR3 expression in a large bladder cancer cohort treated by radical cystectomy: implications for anti-FGFR3 treatment?(†). Eur Urol 2020;78(5):682–7.
[61] Seiler R, Ashab HAD, Erho N, van Rhijn BWG, Winters B, Douglas J, et al. Impact of molecular subtypes in muscle-invasive bladder cancer on predicting response and survival after neoadjuvant chemotherapy. Eur Urol 2017;72(4):544–54.
[62] Loriot Y, Necchi A, Park SH, Garcia-Donas J, Huddart R, Burgess E, et al. Erdafitinib in locally advanced or metastatic urothelial carcinoma. N Engl J Med 2019;381(4):338–48.
[63] Siefker-Radtke AO, Necchi A, Park SH, Js G-D, Huddart RA, Burgess EF, et al. First results from the primary analysis population of the phase 2 study of erdafitinib (ERDA; JNJ-42756493) in patients (pts) with metastatic or unresectable urothelial carcinoma (mUC) and FGFR alterations (FGFRalt). J Clin Oncol 2018;36(15_suppl):4503.
[64] Joerger M, Cassier PA, Penel N, Cathomas R, Richly H, Schostak M, et al. Rogaratinib in patients with advanced urothelial carcinomas prescreened for tumor FGFR mRNA expression and effects of mutations in the FGFR signaling pathway. J Clin Oncol 2018;36(15_suppl):4513.
[65] Nakanishi J, Wada Y, Matsumoto K, Azuma M, Kikuchi K, Ueda S. Overexpression of B7–H1 (PD-L1) significantly associates with tumor grade and postoperative prognosis in human urothelial cancers. Cancer Immunol Immunother 2007;56(8):1173–82.
[66] Boorjian SA, Sheinin Y, Crispen PL, Farmer SA, Lohse CM, Kuntz SM, et al. T-cell coregulatory molecule expression in urothelial cell carcinoma: clinicopathologic correlations and association with survival. Clin Cancer Res 2008;14(15):4800–8.
[67] Rosenberg JE, Hoffman-Censits J, Powles T, van der Heijden MS, Balar AV, Necchi A, et al. Atezolizumab in patients with locally advanced and metastatic urothelial carcinoma who have progressed following treatment with platinum-based chemotherapy: a single-arm, multicentre, phase 2 trial. Lancet 2016;387(10031):1909–20.